Available online at www.sciencedirect.com
SCIENCE DIRECT
Journal of volcanology and geothermal research
ELSEVIER
Journal of Volcanology and Geothermal Research 153 (2006) 21–36
www.elsevier.com/locate/jvolgeores

# Attenuation in gas-charged magma

L. Collier [a], J.W. Neuberg [a,*], N. Lensky [b], V. Lyakhovsky [b], O. Navon [c]

[a] *Department of Earth Sciences, University of Leeds, Leeds, U.K.*
[b] *Geological Survey of Israel, Jerusalem, Israel*
[c] *Institute of Earth Sciences, The Hebrew University of Jerusalem, Jerusalem, Israel*

Received 11 May 2004; received in revised form 12 April 2005; accepted 17 August 2005
Available online 6 January 2006

**Abstract**

Low frequency seismic events observed on volcanoes, such as Soufriere Hills Volcano, Montserrat, are thought to be caused by a resonating system. The modelling of seismic waves in gas-charged magma is critical for the understanding of seismic resonance effects in conduits, dykes and cracks. Seismic attenuation, which depends mainly on magma viscosity, gas and crystal content, is an essential factor in such modelling attempts. So far only two-phase gas–melt systems with the assumption of no diffusion and transport of volatiles between the melt and the gas bubbles have been considered. In this study, we develop a method of quantifying attenuation within gas-charged magma, including the effects of diffusion and exsolution of gas into the bubbles. The results show that by including such bubble growth processes attenuation levels are increased within magma. The resulting complex behaviour of attenuation with pressure and frequency indicates that two factors are controlling attenuation, the first due to viscous hindrance or the melt, and the second due diffusion processes. The level of attenuation within a gas-charged magma conduit suggests an upper limit on the length of a resonating conduit section of just a few hundred meters.


*Keywords:* attenuation; low frequency events; resonance; bubble growth; magma

## 1. Introduction

Seismic signals of special interest associated with many volcanoes are long period and hybrid events (Lahr et al., 1994). These events have characteristic signatures of short, high frequency onsets (which are more prominent in hybrids) followed by a low frequency coda (0.2–5 Hz) making them distinct from other seismic signals observed on volcanoes, e.g. rockfalls and volcano-tectonic events. Due to their similar low frequency content, within this paper we group long period and hybrid events together and name them Low Frequency (LF) events.

Swarms of LF events have occurred before a number of eruptions, e.g. 1989–1990 eruption of Redoubt, Alaska (Stephens et al., 1994) and 1996 Soufrière Hills Volcano, Montserrat, W.I. (Miller et al., 1998), and, therefore, have often been considered a useful indicator of impending eruptions. At Soufrière Hills Volcano specifically, LF swarms correlate well with observed tilt cycles (Voight et al., 1998) which, in turn, indicate the pressurisation and depressurisation of the volcanic system. In general, LF events play an important role in any attempt to assess the state of a volcanic system.

One of the interesting features of LF events are their strongly peaked spectra. These ‘peaks’ are thought to

* Corresponding author. Tel.: +44 113 343 6769; fax: +44 113 343 5259.
*E-mail address:* locko@earth.leeds.ac.uk (J.W. Neuberg).

0377-0273/$ - see front matter © 2005 Elsevier B.V. All rights reserved.
doi:10.1016/j.jvolgeores.2005.08.009

represent the eigenfrequencies of a resonating system involving the interaction of a fluid with a solid medium (Chouet, 1996a; Neuberg, 2000). A number of resonating models explain the formation of LF events, however the crack model (Aki et al., 1977; Chouet, 1988) and the resonating conduit model (Neuberg, 2000) explain best the observed seismic data and, at the same time, allow transport of mass (e.g. magma or ash–gas mixtures) within the volcanic system.

The crack model was first suggested by Aki et al. (1977) and has since been thoroughly investigated using finite difference methods and by comparing the model to observed volcanic data, e.g. Redoubt, Alaska (Chouet et al., 1994). A pressure pulse in the fluid-filled crack generates a slow wave called a 'crack wave,' and the spectral peaks calculated from this model represent the longitudinal and lateral modes of resonance of the crack. The fluid is assumed to be homogeneous throughout the crack, however, its exact composition is unknown and suggestions range from a mixture of gases (e.g. $H_2O$ and $SO_2$) or an ash–gas mixture, to magma (Morrissey and Chouet, 2001). The high gas content in these fluids greatly reduces the seismic velocity of the wave allowing the dimensions of the crack to be of realistic size within the volcano, e.g. crack length 300 m, crack width 150 m and a crack aperture of 0.1 m (Chouet et al., 1994). At present, however, there is no direct evidence of the existence of such large uniform cracks within volcanoes.

Alternatively, a magma conduit is used as a resonator with much greater dimensions compared to the crack model. Conduits, whether a cylindrical pipe or a dyke-like structure, are the main route for magma ascent from the chamber at depth to the surface, and typical conduit dimensions for Soufrière Hills Volcano is a length of up to a few kilometres, and a diameter of around 30 m (Barclay et al., 1998; Sparks et al., 2000). Using finite difference methods it has been shown that conduits are potential resonators (Neuberg, 2000) producing seismic signals consistent with observed LF events on Soufrière Hills Volcano, Montserrat. In contrast to the crack models, the conduit models are filled with a melt, gas and crystal mixture with properties that are depth-dependent (Neuberg and O'Gorman, 2002) and also time-dependent (Sturton and Neuberg, 2003).

Magma is highly viscous and above the nucleation depth contains gas in the form of bubbles. Chouet (1996a) suggests that such a gas-charged magma is highly attenuative, very quickly damping any seismic waves propagating within it. Although attenuation may be determined from studying the amplitude decay of seismic waves with distance from their source, it may also be calculated from the material properties of the medium through which the waves pass. In this study we investigate and quantify attenuation in a gas-charged magma to assess whether a wave can travel within such a magma long enough to sustain resonance, allowing the formation of LF events.

Previous studies of attenuation in bubbly liquids have assumed that the bubbles change size by ideal gas expansion and contraction alone, i.e. there is no transport of volatiles from the liquid to the bubbles, and vice versa (Commander and Prosperetti, 1989). Particularly for magma with small gas bubbles, bubble growth experiments have shown that when the bubbly melt is subjected to a sudden pressure drop the bubbles grow not only due to gas expansion, but also due to the exsolution of volatiles (e.g. water) from the melt into the bubbles, increasing the overall bubble mass (Navon et al., 1998). To model accurately the attenuation in such a magma, we extend the approach of Commander and Prosperetti (1989) and develop a method of quantifying attenuation that includes the effects of the transport of volatiles to and from the bubbles, and also allows us to consider a finite separation of bubbles. We then apply this method to investigate attenuation within a magma conduit, using parameters that match those of Soufrière Hills Volcano, Montserrat, and discuss the implications for wave propagation and resonance within magma conduits.

## 2. Quantification of attenuation

Attenuation of seismic waves is generally quantified through the parameter $Q$. In the literature different definitions are used depending on the conditions of application. The most frequently used definition is given by the dimensionless measure of the internal friction (e.g. Aki and Richards, 2002)

$$Q_{\mathrm{h}} = \frac{2\pi E_{\max}}{\Delta E}, \tag{1}$$

where $E_{\max}$ is the maximum elastic energy stored during a cycle at the frequency of interest and $\Delta E$ is the energy dissipated in one cycle. The more energy that is lost in one cycle, the greater the attenuation and the lower $Q$ is. This definition can equally be written in terms of the attenuation coefficient, $\alpha$,

$$Q_{\mathrm{h}} = \frac{\omega}{2v_{\mathrm{ph}}\alpha} \tag{2}$$

$v_{\mathrm{ph}}$ is the phase velocity of the wave at the frequency of interest, $\omega = 2\pi f$ (the angular frequency). Through the

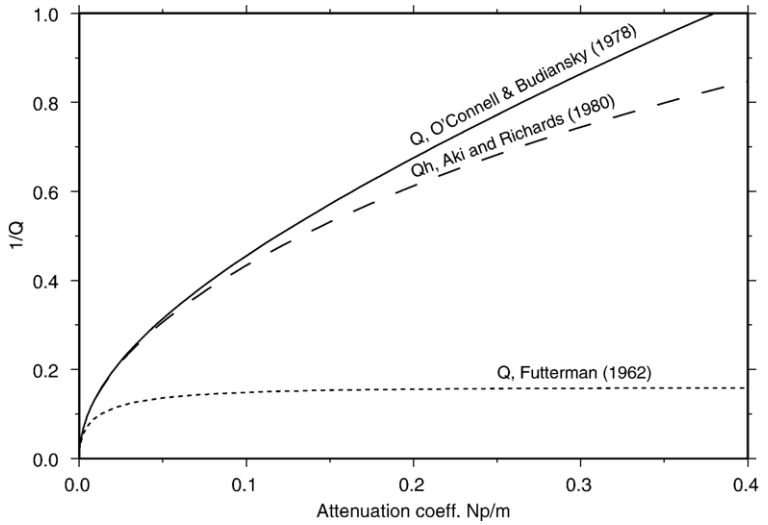


Fig. 1. Comparison of the different definitions of $Q$. High $Q$ definition, $Q_h$, Eq. (2). The Futterman (1962) $Q$ definition, Eq. (4), and the full $Q$ definition, Eq. (6). The inverse of $Q$ (attenuation) is plotted against the attenuation coefficient, $\alpha$(1 Np=20/ln(10) dB). As attenuation increases ($1/Q$ close to 1), the three solutions diverge.

attenuation coefficient, $\alpha$, the amplitude of a propagating wave as a function of distance can be determined,

$$A(x) = A_o e^{-\alpha x}, \tag{3}$$

where $A(x)$ is the amplitude of the wave after travelling distance $x$ within the damping medium and $A_o$ is the initial amplitude of the wave.

We have labelled these definitions with the subscript 'h,' as they are approximations valid at low attenuation levels (high $Q$) (Kjartansson, 1979), i.e. when $Q \gg 1$, or $1/Q \ll 1$ (Fig. 1). Within a gas-charged magma we expect high attenuation (low $Q$) and therefore, these definitions are not suitable.

A further definition of $Q$ derived from Eq. (1), is quoted by Futterman (1962),

$$Q = \frac{2\pi}{1 - \exp\left(\frac{-4\pi\alpha v_{ph}}{\omega}\right)}. \tag{4}$$

When the attenuation is strong (low $Q$), this definition tends to $2\pi$ (Fig. 1) making it also impractical for the conditions of interest in this study.

An alternative definition for $Q$, in terms of energy, is given by O'Connell and Budiansky (1978),

$$Q = \frac{4\pi E_{ave}}{\Delta E}, \tag{5}$$

where $E_{ave}$ is the average energy in one cycle. It can be re-written as

$$Q = \frac{\omega}{2v_{ph}\alpha} - \frac{\alpha v_{ph}}{2\omega}. \tag{6}$$

This definition can be applied for systems with all values of $Q$, and tends to $Q_h$ if the attenuation is low, as $2E_{ave} \rightarrow E_{max}$ and $\alpha v_{ph}/2\omega \rightarrow 0$ (Fig. 1).

Throughout this paper we use $Q$ definitions based on Eq. (5) as it accurately represents attenuation at all attenuation levels. In many applications $Q$ is not directly determined from the energy of the wave but in terms of the material properties by which the wave is attenuated. The constitutive equation of a viscoelastic medium can be written as (Christensen, 1971),

$$\sigma = \left(\kappa + \frac{2}{3}\mu + i\omega\left(\lambda + \frac{2}{3}\eta\right)\right)\varepsilon_A e^{i\omega t}$$
$$= M(\omega)\varepsilon_A e^{i\omega t}. \tag{7}$$

Here $\sigma$ is the applied stress, and $=_A e^{i\omega t}$ is the resulting strain of the system. $M(\omega)$ is the complex modulus of the material, with the real part containing the shear modulus and the second lamè parameter, $\mu$ and $\kappa$, respectively, and the imaginary part with the shear viscosity and the second coefficient of viscosity, $\eta$ and $\lambda$, respectively. The volume viscosity is related to these viscosities through the following relationship,

$$\zeta = \lambda + \frac{2}{3}\eta, \tag{8}$$

where the shear viscosity ($\eta$) is the viscosity opposing shear stresses, the second coefficient ($\lambda$) is the viscosity opposing pure expansion changes, and the volume viscosity ($\zeta$) is the viscosity opposing volume changes, which includes shear and expansion stresses (Christensen, 1971). These viscosities are analogous to the elas-

tic moduli, where the volume modulus ($B$) of the material is,

$$B = \kappa + \frac{2}{3}\mu, \tag{9}$$

analogous to the volume viscosity ($\zeta$).

The constitutive equation (Eq. (7)) can also be expressed in terms of the phase lag between applied stress and resulting strain ($\psi$),

$$\sigma = |M(\omega)|\varepsilon_A e^{i\omega t-\psi} \tag{10}$$

where $\psi$ is defined as

$$\tan\psi = \frac{\Im[M(\omega)]}{\Re[M(\omega)]} = \frac{\omega\zeta}{B}. \tag{11}$$

Here the volume viscosity, $\zeta$, is given by Eq. (8) and the volume modulus, $B$, is given by Eq. (9). $Q$ can be determined from the ratio of real to imaginary parts of the complex modulus, $M(\omega)$ (O'Connell and Budiansky, 1978; Christensen, 1971),

$$Q = \frac{\Re[M(\omega)]}{\Im[M(\omega)]} = \frac{B}{\omega\zeta} = \frac{1}{\tan\psi}. \tag{12}$$

This definition of $Q$ is equivalent to the definition in Eq. (5), and can therefore be used for conditions of high attenuation. Eq. (12) illustrates that $Q$ is directly dependent on the properties of the attenuating material; however, if these properties are unknown, $Q$ can still be determined through the phase lag, $\psi$.

## 3. Attenuation in bubbly liquids

### 3.1. Previous work

The classic work investigating the effects of attenuation due to bubbly liquids was that by Commander and Prosperetti (1989). They used the Van Wijngaarden–Papanicolaou model of propagation of nonlinear pressure waves in bubbly liquids (Van Wijngaarden, 1968) to determine an expression for the attenuation coefficient, $\alpha$, thereby quantifying attenuation. They assumed small amplitude oscillations, infinite separation of the bubbles, a Newtonian liquid surrounding the bubbles, and no transport of volatiles between the liquid and the bubbles. This implies that any change in the size of the bubbles, or in the gas volume fraction of the medium, is due to the expansion of an ideal gas. For future clarity, this process of ideal gas expansion and contraction will be referred to as 'bubble growth by expansion.' At frequencies well below the natural frequency of the bubble system, $\omega_o$, they determined an expression for the complex velocity of the wave travelling in the bubbly liquid ($v_b$):

$$\frac{v_m^2}{v_b^2} \approx 1 + 4\pi v_m^2 \frac{Rn}{\omega_o^2}\left(1 - \frac{2ib\omega}{w_o^2}\right), \tag{13}$$

where $v_m$ is the velocity of the wave within the liquid melt, $n$ is the bubble number density and $R$ is the bubble radius (typical values in Table 1). The natural

Table 1
Parameters and constants used in the runs unless otherwise stated

| Parameter | Symbol | Value | Reference |
|---|---|---|---|
| Melt density | $\rho_m$ | 2300 kg m$^{-3}$ | Rivers and Carmichael (1987) |
| Crystal density ($An_{53}$) | $\rho_c$ | 2680 kg m$^{-3}$ | Carmichael (1990) |
| Rock density | $\rho_r$ | 2500 kg m$^{-3}$ | Melnik and Sparks (1999) |
| Melt $P$-wave velocity | $v_m$ | 2354 m s$^{-1}$ | Rivers and Carmichael (1987) |
| Crystal $P$-wave velocity | $v_c$ | 6570 m s$^{-1}$ | Carmichael (1990) |
| Ideal gas constant | $C_g$ | 8.3145 J (mol K)$^{-1}$ | |
| Molecular weight of $H_20$ | $m$ | 0.018 kg mol$^{-1}$ | |
| Magma temperature | $T$ | 1100 K | Devine et al. (1998) |
| Total water content | $c_o$ | 0.04 | Barclay et al. (1998) |
| Ratio of specific heats | $\gamma$ | 1.33 | general constant |
| Thermal diffusivity constants | $C_1$ | $5.2810\times10^{-5}$ N s$^{-1}$ K$^{-2}$ | |
| | $C_2$ | 0.01165 N s$^{-1}$ K$^{-1}$ | Prosperetti et al. (1988) |
| Surface tension | $\Gamma$ | 0.05 N m$^{-1}$ | Lyakhovsky et al. (1996) |
| Bubble no. density | $n$ | $10^{12}$ ($10^{10}$–$10^{14}$) m$^{-3}$ | Navon et al. (1998) |
| Waves frequency | $f$ | 1 (0.1–10) Hz | Neuberg et al. (1998) |
| Diffusivity | $D$ | $10^{-11}$ ($10^{-13}$–$10^{-10}$) m$^2$ s$^{-1}$ | Zhang and Behrens (2000) |
| Solubility constant | $K_h$ | $4.11\times10^{-6}$ Pa$^{-1/2}$ | Burnham (1975) |
| Amplitude of wave | $P_A$ | 0.1 MPa | – |

Values are chosen to represent magma from Soufrière Hills Volcano, Montserrat, W.I.

frequency of the bubbles ($\omega_o$) and the damping constant ($b$) are given by,

$$\omega_o^2 = \frac{3P_{amb}}{\rho_m R^2} \tag{14}$$

$$b = \frac{\gamma - 1}{10\gamma}\frac{P_{amb}}{\rho_m D_T} + \frac{2\eta_m}{\rho_m R^2}, \tag{15}$$

respectively. These definitions were formulated to illustrate the similarity of the response to that of a simple harmonic oscillator. Within the volcano, $P_{amb}$ is the ambient pressure of the magma, $\rho_m$ and $\eta_m$ are the density and the shear viscosity of the liquid melt phase respectively, $D_T$ is the thermal diffusivity of the gas, and $\gamma$ is its specific heat ratio. The thermal diffusivity can be determined using the expression (Prosperetti et al., 1988),

$$D_T = \frac{(\gamma - 1)k_g(T)T}{\gamma P_{amb}}, \tag{16}$$

where $k_g(T) = C_1T + C_2$ gives the dependence of the thermal conductivity of the gas on $T$, the ambient temperature (Table 1).

These expressions were developed as a 'low frequency approximation' assuming that the frequencies of interest are well below the resonant frequency, $\omega_o$. For a typical ambient pressure of $P_{amb} = 60$ MPa and a bubble of radius, $R \approx 10^{-5}$ m, the natural resonance frequency of bubbles within a rhyolitic melt is $\omega_o = 10^7$ rad/s (Table 1). This is well above the seismic frequencies of interest, and the 'low frequency approximation' discussed above, matches the full solutions (Eqs. (32) and (33)): Commander and Prosperetti, 1989) valid for all frequencies (Fig. 2). Care must be taken, however, when using these low frequency approximations, as they can differ from the full solutions (Eqs. (32) and (33)): Commander and Prosperetti, 1989) even though the frequencies of interest are far below the bubble resonance frequency, $\omega_o$ (P. Jousset, personal communication, 2004). An example of such conditions are those of basaltic magma, where the bubbles are larger (typically $10^{-3}$ m) and the shear viscosity is lower ($\approx$ 10 Pa s Chouet, 1996b) compared to the rhyolite conditions assumed here ($R \approx 10^{-5}$ m, $\eta_m = 10^6$ Pa s). For basaltic magma, $\omega_o \approx 10^4$ rad/s, and the seismic frequencies of interest are still, $\omega \ll \omega_o$, but the low frequency approximations can be seen to differ from the full solutions (Fig. 2).

To determine $Q$ we use the real and imaginary parts of the complex velocity, $v_b^2$ (Eq. (13)), as this is equivalent to the definition in Eq. (12), and therefore valid for all values of $Q$ (O'Connell and Budiansky, 1978):

$$Q = \frac{\Re(M(\omega))}{\Im(M(\omega))} = \frac{\Re(v_b^2)}{\Im(v_b^2)} = \frac{1 + 4\pi v_m^2 \frac{Rn}{\omega_o^2}}{8b\omega\pi v_m^2 \frac{Rn}{\omega_o^4}}. \tag{17}$$

### 3.2. Attenuation model

Throughout this study we approach the quantification of attenuation in bubbly liquids from a different angle than Commander and Prosperetti (1989). Our main aim is to include the effects of volatile transport to and from the bubbles and investigate the resultant effects on attenuation. When a bubble–melt system,

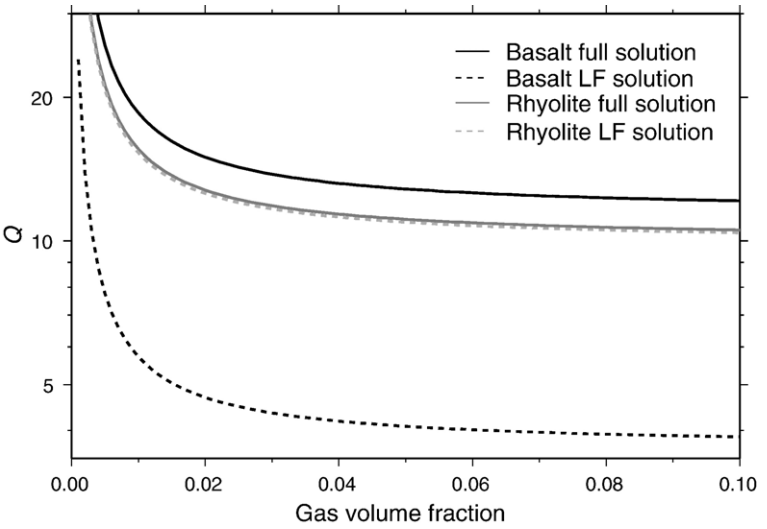


Fig. 2. Comparison between the full solutions and the low frequency approximations of Commander and Prosperetti (1989). Shown are the results for basaltic magma, $R \approx 10^{-3}$ m and $\eta_m \approx 10$ Pa s, and for rhyolitic magma, $R \approx 10^{-5}$ m and $\eta_m \approx 10^6$ Pa s (other parameters as in Table 1).

initially in equilibrium, is decompressed, the amount of water that can remain in solution in the melt decreases ($c_m$). To allow equilibrium to be restored, water diffuses towards the bubble–melt boundaries and exsolves into the bubbles, increasing their mass. If pressure is then increased, the opposite process occurs, water re-dissolves into the melt surrounding the bubbles and then, due to the concentration gradient produced, diffuses away into the surrounding melt. Later in this paper, this process will be called 'bubble growth by diffusion' regardless of whether the bubble is growing or shrinking. Within this paper we will consider this process reversible, however it has been shown that when such a system is subjected to sustained pressure oscillations the slight irreversibility of the diffusion process causes an overall increase in bubble size with time, called rectified diffusion (Brodsky et al., 1998). The time required for this net growth to be noticeable, however, is much greater than the timescales of seismic waves as modeled here, and is therefore neglected.

We model the melt as a Newtonian liquid, which is able to sustain volatiles dissolved within it. Melt can exhibit non-linear viscoelastic behaviour; however, we use the Newtonian assumption to allow clearer comparison with the work of Commander and Prosperetti (1989) and to simplify the theory involved. In this instance, we assume water is the only volatile in the system and use the approximation of Burnham (1975) to determine the solubility as a function of pressure:

$$c_m \approx K_h \sqrt{P_{amb}}. \tag{18}$$

Here $c_m$ is the concentration of water dissolved in the melt, $P_{amb}$ is the ambient pressure and, $K_h$ is the solubility constant (Table 1). As pressure increases, more water dissolves in the melt, and the radius of the gas bubbles decreases, reducing the gas volume fraction,

$$R^3 = \frac{(c_o - c_m)\rho_m S_o^3}{\rho_g}, \tag{19}$$

where $\rho_m$ is the density of the melt, $\rho_g$ is the gas density, $R$ is the bubble radius, $S_o = 3/(4\pi n)$ is the radius of the melt shell when the bubble vanishes (Fig. 3) and $c_o$ is the total water concentration in the system. The pressure at which all water is just dissolved in the melt, i.e. when $c_m = c_o$, is called the saturation pressure ($P_{sat}$). We assume that prior to the passing of the applied wave, the bubble–melt system is in full equilibrium with the ambient pressure.

We model the shear viscosity of the melt as being dependent on its temperature and on the water content dissolved within it, as described by Hess and Dingwell (1996) for rhyolitic melts. Although the overall magma composition of Soufrière Hills Volcano, Montserrat, is andesite, due to the crystal content the composition of the remaining melt is close to that of rhyolite (Murphy et al., 1998), making these characteristics valid for use in this model.

We model how the bubbles react to the pressure oscillations of a passing seismic wave,

$$P_{amb} = P_o - P_A \sin\omega t, \tag{20}$$

by using the numerical bubble growth code derived by Lyakhovsky et al. (1996). This approach assumes that the only variation felt by the bubbles with time are the pressure oscillations of the wave ($P_A \sin \omega t$). The average pressure, $P_o$ remains constant, and as the am-

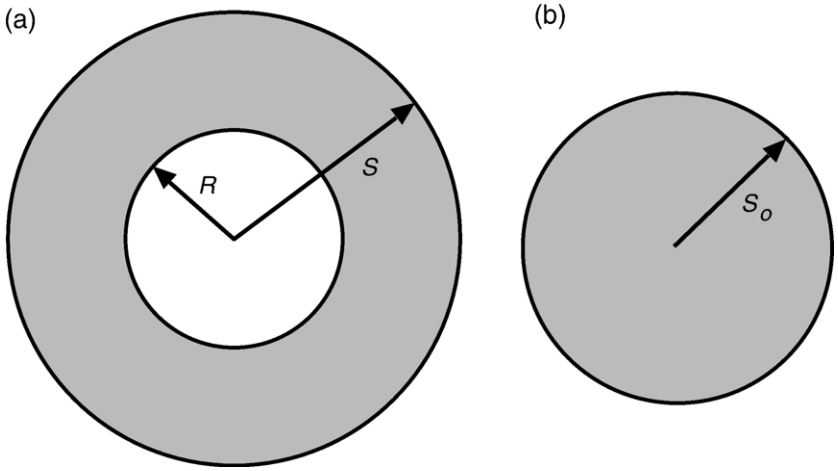


Fig. 3. (a) Each bubble of radius, $R$, interacts with a spherical shell of melt which is assumed to be spherical with radius, $S$. The total volume of the shell is $V = \frac{4}{3}\pi S^3$. (b) The volume of melt in the shell is $V_m = \frac{4}{3}\pi(S^3 - R^3) = \frac{4}{3}\pi S_o^3$, where $S_o$ is the radius of the melt shell when the bubble vanishes, as shown in (b).

plitude of the pressure oscillations are small ($P_A < P_o$) the temporal variation of dissolved water content ($c_m$) and viscosity can be neglected (Lyakhovsky et al., 1996). The model also assumes no interaction between individual bubbles, which is valid as long as the volume of melt in the cell is greater than the gas volume, i.e. $S_o^3 > R^3$ or the gas volume fraction, $\chi_g < 50\%$ (Fig. 3). The effective shear viscosity of the surrounding melt can be reasonably represented by the viscosity at the bubble–melt interface (Lensky et al., 2001). The numerical method solves simultaneously for Fick's law of diffusion,

$$\frac{\partial c_m}{\partial r} + \frac{\partial c_m}{\partial r} v_r = \frac{1}{r^2} \frac{\partial}{\partial r} \left( Dr^2 \frac{\partial c_m}{\partial r} \right), \tag{21}$$

where $r$ is the radial coordinate, $v_r$ is the velocity in the radial direction as the system oscillates, and $D$ is the diffusivity of water within the melt, and for the balance of pressures within the system,

$$P_g - P_{amb} = 4\eta_m \dot{R} \left( \frac{1}{R} + \frac{R^2}{S^3} \right). \tag{22}$$

If the bubbles can be reasonably considered to have infinite separation ($S_o^3 \gg R^3$), this simplifies to

$$P_g - P_{amb} = 4\eta_m \dot{R} \left( \frac{1}{R} \right). \tag{23}$$

If the pressure of the gas in the bubbles, $P_g$, and the ambient pressure, $P_{amb}$, are known along with the bubble radius, $R$, we can determine the rate of bubble growth, $\dot{R}$ and, hence, the change in size of the bubbles for each time-step. As the bubbles change size we expect the gas pressure within the bubbles to change as well. This is modelled through the rate of change of the gas density,

$$\frac{\partial \rho_g}{\partial t} = \frac{3D\rho_m}{R} \left( \frac{\partial c_m}{\partial r} \right)_R - \frac{3\rho_g \dot{R}}{R}. \tag{24}$$

The first term on the right-hand side shows the variation in $\rho_g$ due to changes in mass of the bubbles, i.e. due to growth by diffusion. The second term is the change in $\rho_g$ due to ideal gas expansion.

We determine the resultant strain rate,·, of the system from the bubble oscillations calculated numerically (Lensky et al., 2002):

$$\dot{\varepsilon} = \frac{3R^2 \dot{R}}{\left(R^3 + S_o^3\right)}, \tag{25}$$

and hence, the phase lag of the strain rate behind the stress can be measured ($\phi$), assuming that the response of the bubble–melt system is the same as that of the bubbles, i.e. melt is effectively incompressible. However, it is known that melt is compressible to a certain degree, as acoustic $P$-waves travel through melt with a finite velocity ($v_m \approx 3000$ m s$^{-1}$ Rivers and Carmichael, 1987). The deformation strain of melt related to the pressure oscillation ($P_A$) is given by,

$$\varepsilon_m = \frac{P_A}{\rho_m v_m^2} \tag{26}$$

where $v_m$ is the velocity of acoustic waves within the melt. The assumption that melt compressibility is negligible is valid as long as,

$$\varepsilon \gg \varepsilon_m, \tag{27}$$

where  is the strain of the system due to the effect of the bubbles, determined through Eq. (25). Within gas-charged magma this assumption is seen to hold except at very high pressures close to the saturation pressure, where the gas volume fraction is low. Hence, the strain rate of the bubble–melt system can be reasonably described by Eq. (25). As strain rate is the time derivative of the strain the phase lag of the resultant strain behind the stress can be found through, $\psi = \phi - \pi/2$, hence, $Q$ may be determined and quantified (Eq. (12)).

In summary, we use the numerical method of Lyakhovsky et al. (1996) to solve for the bubble radius, and the rate of bubble growth at each time-step using Eqs. (21)–(24). The bubble radius, $R$, and the rate of change of bubble radius, $\dot{R}$ are used to determine the strain rate ($\dot{\varepsilon}$) at each time-step, thereby allowing us to estimate the phase lag of the resultant strain rate ($\phi$) behind the applied stress wave (Eq. (20)). This phase lag is then converted to the phase lag of strain ($\psi$) which is then used to determine $Q$ for the system (Eq. (12)).

Using this method we can investigate the attenuation of a bubbly liquid in which the bubbles have a finite separation (Eq. (22)), thus extending the range of gas volume fractions for which $Q$ can be determined. We can also investigate the effects of including bubble growth by diffusion as well as by ideal gas expansion.

To verify that this 'phase lag method' can reproduce the results of Commander and Prosperetti (1989) we solved for the case of no diffusion, i.e. no transport of volatiles between the bubbles and the melt ($D = 0$), and infinite separation between bubbles (Eq. (23)). The results in Fig. 4 demonstrate that the two methods match very well at pressures and frequencies representative of conditions within gas-charged magmas (Table 1). We have therefore verified that this method accurately reproduces the results of previous methods,

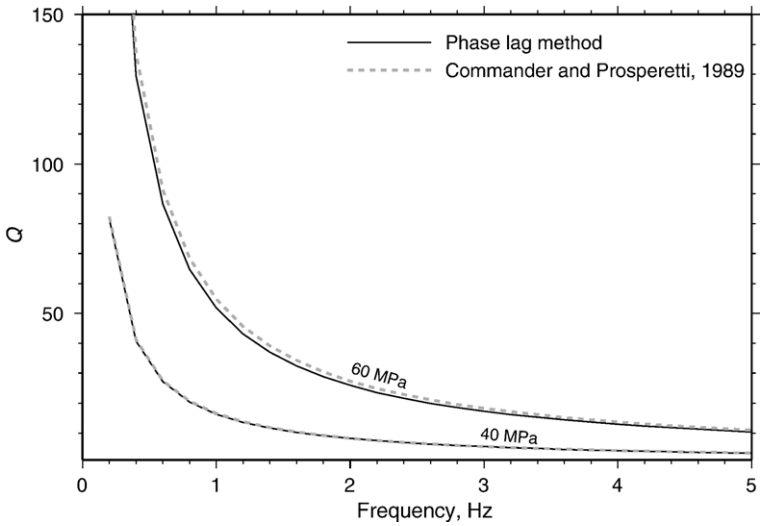


Fig. 4. Comparison of the phase lag method developed within this paper (thin solid line) with the method of Commander and Prosperetti (1989) (thick dashed line), under the conditions of infinite separation of bubbles, no diffusion growth ($D=0$) at $P_o=40/60$ MPa ($n=10^{13}$ m$^{-3}$).

and we can now extend the method to look at conditions previously not modelled.

## 4. Results

Firstly, we consider the effects of allowing a finite distance between bubbles, instead of assuming infinite separation as in Commander and Prosperetti (1989). Fig. 5 shows the variation of $Q$ with pressure, and hence, with gas volume fraction and water concentration in the melt. Using the input parameters as listed in Table 1, the figure demonstrates that the infinite separation assumption is only fully valid at high pressures, approaching the saturation pressure (in this case $P_{sat} \approx 90$ MPa), i.e. where the bubbles are small and the gas volume fraction is low. At lower pressures the two solutions diverge gradually, illustrating the breakdown of the infinite separation assumption as the bubbles increase in size. Therefore, by considering finite separation we are able to quantify attenuation ($Q$) for higher gas volume fractions (lower pressures) than in the method of Commander and Prosperetti (1989).

Fig. 6 illustrates the behaviour of $Q$ with increasing initial ambient pressure, $P_o$, including the effects of

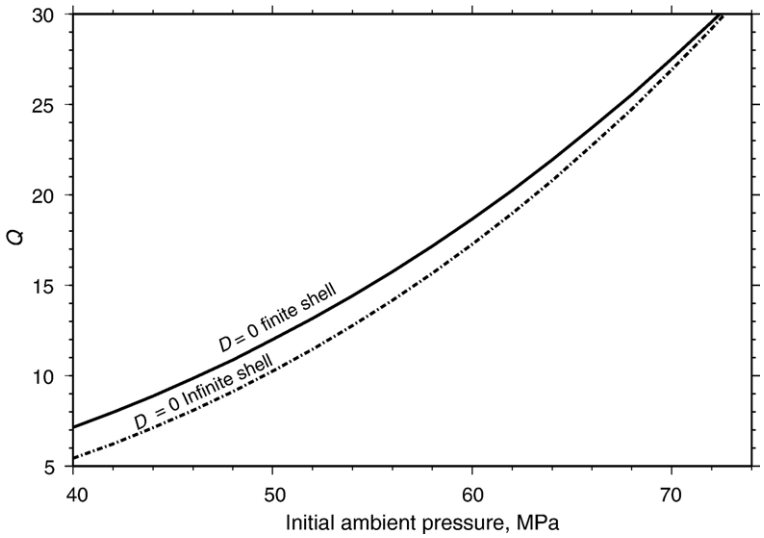


Fig. 5. Results of $Q$ varying with pressure ($P_o$) as determined by the phase lag method under the conditions of no growth by diffusion ($D=0$). Comparison of finite bubble separations (Eq. (22)) with infinite separations (Eq. (23)). Input parameters as in Table 1, with $n=10^{13}$ m$^{-3}$ and $f=1$ Hz.

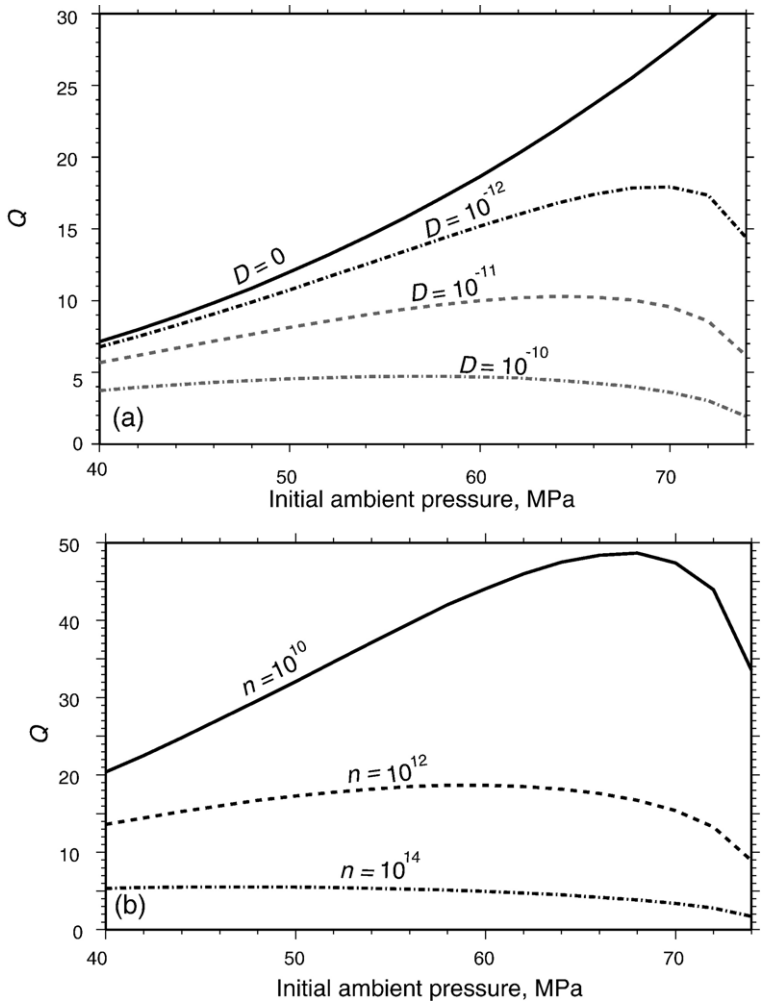


Fig. 6. (a) Dependence of $Q$ on initial ambient pressure ($P_o$) for different values of diffusivity, $D$. As $D$ decreases the overall $Q$ values decrease ($n=10^{13}$ m$^{-3}$, $f=1$ Hz). (b) Variation of $Q$ for different bubble number densities, $n$. $Q$ is greater for large $n$, i.e. small bubbles, than for low $n$, large bubbles. Input parameters as in Table 1, $D=10^{-11}$ m$^2$ s$^{-1}$, and $f=1$ Hz.

diffusion growth (Diffusivity: $D>0$). Input parameters are as listed in Table 1, unless otherwise stated. Overall, when the diffusivity, $D$, is increased the value of $Q$ decreases. By increasing diffusivity ($D$), more diffusion and greater transport of water between the melt and the bubbles occurs, i.e. we have more growth by diffusion. This increased degree of bubble growth causes more attenuation and overall reduces $Q$. These results clearly imply that including bubble growth by diffusion causes more attenuation (lower $Q$) than growth by gas expansion alone ($D=0$).

When the diffusivity, $D=0$, we have bubble growth by gas expansion alone (as in Commander and Prosperetti (1989)). As we increase the ambient pressure of the magma (increase $P_o$), the equilibrium amount of water dissolved in the melt ($c_m$) is increased (Eq. (18)) and the equilibrium bubble size prior to the passing of the wave is reduced (Eq. (19)). The increase in dissolved water content ($c_m$) causes the shear viscosity of the melt to decrease (Hess and Dingwell, 1996). As the initial ambient pressure ($P_o$) is increased, $Q$ is observed to increase in this case ($D=0$) due to the decrease in viscous hindrance caused by the surrounding melt (Fig. 6).

However, when we allow bubbles to grow by diffusion ($D>0$), $Q$ decreases at higher pressures (Fig. 6). By including diffusive growth, we have introduced a second factor which influences attenuation within the bubbly liquid. As shown in Eq. (24), diffusion becomes more effective as bubbles size decreases. This is the case at high pressures, close to saturation and hence, diffusion is highly efficient causing stronger attenuation and lower $Q$ values.

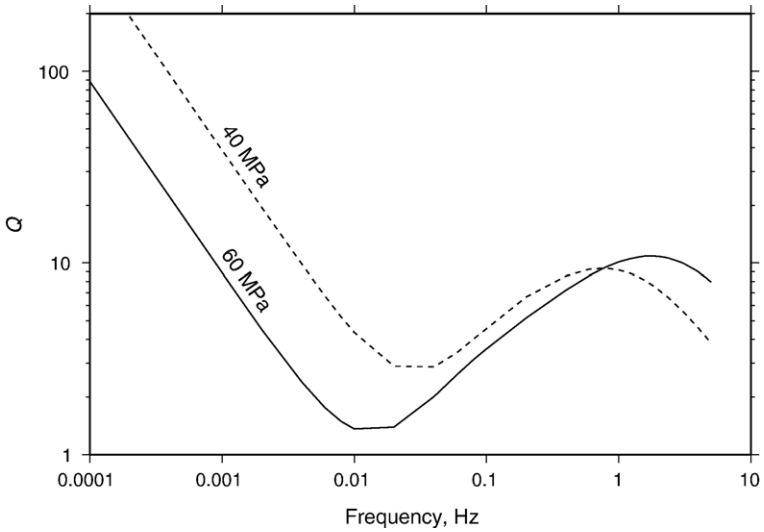


Fig. 7. Dependence of $Q$ on the frequency of the wave at two initial ambient pressures ($P_o$=40/60 MPa). If we had growth by gas expansion alone, $Q$ would decrease with increasing frequency (Fig. 4), though by including growth by diffusion the $Q$ behaviour becomes more complex. Input parameters as in Table 1, with $n=10^{13}$ m$^{-3}$ and $D=10^{-11}$ m$^2$ s$^{-1}$.

A further factor observed to have a noticeable affect on attenuation, and $Q$, is the bubble number density, $n$. The density of bubbles directly controls the size of the bubbles (through $S_o$ and Eq. (19)). At a given pressure for a high bubble number density, $R$ is relatively small and for a low bubble number density, $R$ is relatively large. Through its effect on $R$, the bubble number density determines the effectiveness of diffusion and its ability to attenuate waves and lower $Q$ (Fig. 6 (b)). This variation of $Q$ with n indicates that further constraint of the bubble number density is required before attenuation within magma can be accurately determined.

Fig. 7 shows how $Q$ varies with frequency. Generally, $Q$ decreases with increasing frequency, for example when growth is by gas expansion alone (Fig. 4). However, when including growth by diffusion ($D>0$), we obtain a different variation of $Q$ with frequency. At very low ($f<0.1$ Hz) and high frequencies ($f>3$ Hz) we obtain a similar decrease of $Q$ with increasing frequency, as in Fig. 4. Though between these limits there is a distinct variation, and $Q$ is observed to increase with increasing frequency (Fig. 7). We explain this difference due to the added affect of bubble growth by diffusion. As when diffusion has time to occur, it causes further attenuation, and hence decreases $Q$.

At low pressures and at high frequencies the variation of $Q$ is dominantly controlled by the variation of the shear viscosity of the melt (which depends on $P_o$) and the hindrance to changes in bubble size it causes. Whereas at higher pressures, or at lower seismic frequencies, the variation of $Q$ is controlled by the diffusion process which becomes more dominant than the viscous hindrance factor. The interaction between these two factors hence, determines the observed complex behaviour of $Q$ with pressure and with frequency.

## 5. Implications for magma conduits and resonance

Neuberg and O'Gorman (2002) and Sturton and Neuberg (2003) modelled magma properties within a stationary gas-charged magma conduit by considering the magmastatic pressure, i.e. the pressure due to the weights of magma above. Here we develop a model similar to that of Neuberg and O'Gorman (2002), but we include an excess viscous pressure to simulate the pressure of magma flowing in a cylindrical magma conduit (Sparks, 1997). We assume a slow ascent rate in a fully established conduit, such that at each depth the bubble–melt system is in full equilibrium prior to the initiation of the oscillating pressure wave (Eq. (20)). Thus as the ambient pressure of the magma ($P_o$) increases with depth, the dissolved water content ($c_m$) correspondingly increases, and the shear viscosity decreases.

The pressure profile is set such that the pressure at the magma chamber depth, 5000 m (Barclay et al., 1998), is given by

$$P_o(5000) = P_{lith} + P_{ex}(5000), \quad (28)$$

where $P_{lith}$ is the lithostatic pressure due to the surrounding country rock, and $P_{ex}(5000)$ is the excess pressure at the chamber depth. This is typically given a range of 0–20 MPa, due to the estimated strengths of

conduit walls (Sparks, 1997). The simple method of Sparks (1997) is used to model the variation of the excess pressure with depth ($P_{ex}(z)$). It assumes the magma flow is incompressible, and that the viscosity of the magma can be reasonably estimated by the viscosity of the melt. This model neglects to include the effects of compressible flow, and shear viscosity varying with bubble and crystal content, which have all been shown to have a noticeable effect on flow dynamics (Papale et al., 1998; Melnik and Sparks, 1999). For this study we do not attempt to model all aspects of conduit flow, we require only a reasonable pressure profile for magma in a conduit, and hence the simple of model of Sparks (1997) suffices. A constant crystal content, however, is included ($\chi_c \approx 40\%$), to enable the density of the magma to be more accurately represented,

$$\rho_b = \rho_m(1 - \chi_g - \chi_c) + \rho_g\chi_g + \rho_c\chi_c. \quad (29)$$

Here $\rho_b$, $\rho_m$, $\rho_g$ and $\rho_c$ are the densities of the bulk magma, melt, gas and crystals respectively, and $\chi_g$ and $\chi_c$ are the volume fractions of gas and crystals contained in the magma. The density of the magma directly influences the seismic velocity within magma, which is a key parameter for seismic wave propagation:

$$\alpha = \sqrt{\frac{B_b}{\rho_b}}, \quad (30)$$

where $B_b$ is the volume modulus of the bulk gas–melt–crystal mixture,

$$\frac{1}{B_b} = \frac{1 - \chi_g - \chi_c}{B_m} + \frac{\chi_g}{P_{amb}} + \frac{\chi_c}{B_c} \quad (31)$$

and $B_m$ and $B_c$ are the volume moduli for the liquid melt phase and for the solid crystal phase, respectively. The volume modulus of the gas phase is taken at the ambient pressure of the magma, $P_{amb}$ (Neuberg and O'Gorman, 2002).

Magma properties, and their variation with depth in a cylindrical magma conduit are illustrated in Fig. 8. As the excess pressure at the chamber depth is increased, $P_{ex}(5000) = 0 \rightarrow 20$ MPa, the overall pressure in the conduit increases, directly altering all the other magma parameters. Specifically, as the excess chamber pressure is increased, the depth at which gas first comes out of solution, forming bubbles (the nucleation depth),

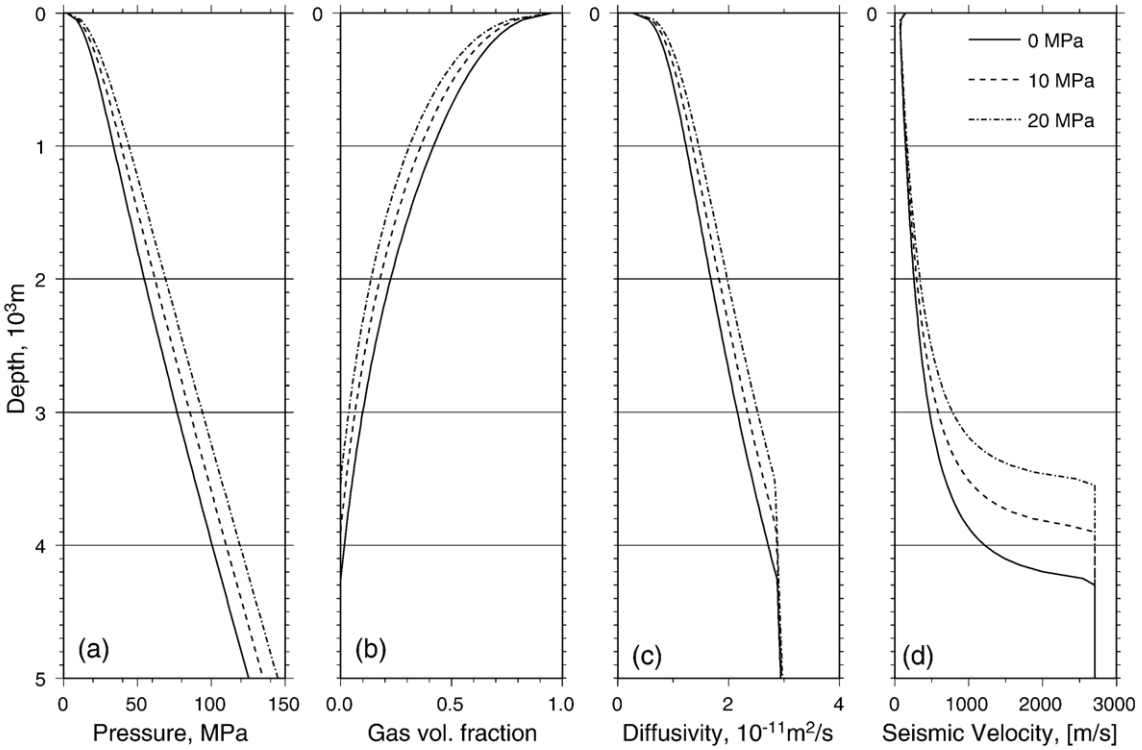


Fig. 8. (a) Pressure profile (Sparks, 1997). (b) Gas volume fraction, zero at the 'nucleation depth.' (c) Diffusivity profile (Zhang and Behrens, 2000). (d) Seismic velocity profile (Eq. (30)). In all plots the lines correspond to different values of $P_{ex}(5000)$, as indicated. Input parameters as in Table 1, with $n = 10^{12}$ m$^{-3}$.

becomes shallower (Fig. 8 (b)). The value of diffusivity in the melt, $D$, has been shown to have a noticeable effect on attenuation. However, diffusivity in magma is not known precisely. The best model available so far is that of Zhang and Behrens (2000) who developed an expression for the dependence of the diffusivity on pressure and temperature. This model is valid for rhyolitic magmas, and as the composition of the melt of Soufrière Hills Volcano, Montserrat, is close to being rhyolitic, this model is used. The resultant diffusivity within the conduit can be seen to change noticeably with depth (Fig. 8 (c)), however the total variation of diffusivity is less than one order of magnitude.

Using these parameters, and the input values in Table 1, Q has been determined within the conduit at a range of wave frequencies (0.1–10 Hz). $Q$ has been calculated below the depth where the gas volume fraction, $\chi_g$, is 50% (the upper red line) as above this level the bubbles interact and the numerical bubble growth code is no longer valid (Lyakhovsky et al., 1996). $Q$ is calculated above the depth at which melt compressibility can be considered to be negligible, i.e. when Eq. (27) is satisfied (the lower solid red line). Also marked on the figures is the nucleation depth for comparison (the dashed red line).

Fig. 9 shows clearly the differences in attenuation in magma conduits when considering bubble growth by gas expansion alone (no diffusion) and when including bubble growth by diffusion (with diffusion). With bubble growth by gas expansion only, $Q$ increases consistently with depth, and decreases with increasing frequency. The maximum $Q$ value found within this conduit is close to 250, which occurs at low frequencies and at depths approaching the nucleation depth (Fig. 9). Whereas when including bubble growth by diffusion, the behaviour of $Q$ with depth (pressure) and frequency is more complex, due to the trade-off between the opposing factors of viscous hindrance and diffusion processes (as in Figs. 6 and 7). The maximum $Q$ value within the conduit is around 20, mid-depth in the conduit (2500 m) and at frequencies around 1 Hz. These high $Q$ values mid-depth in the conduit form a region where resonance could be sustained, allowing us to estimate a depth range where resonance is most likely to occur. By increasing the excess chamber pressure it can be shown that the depths where the maxi-

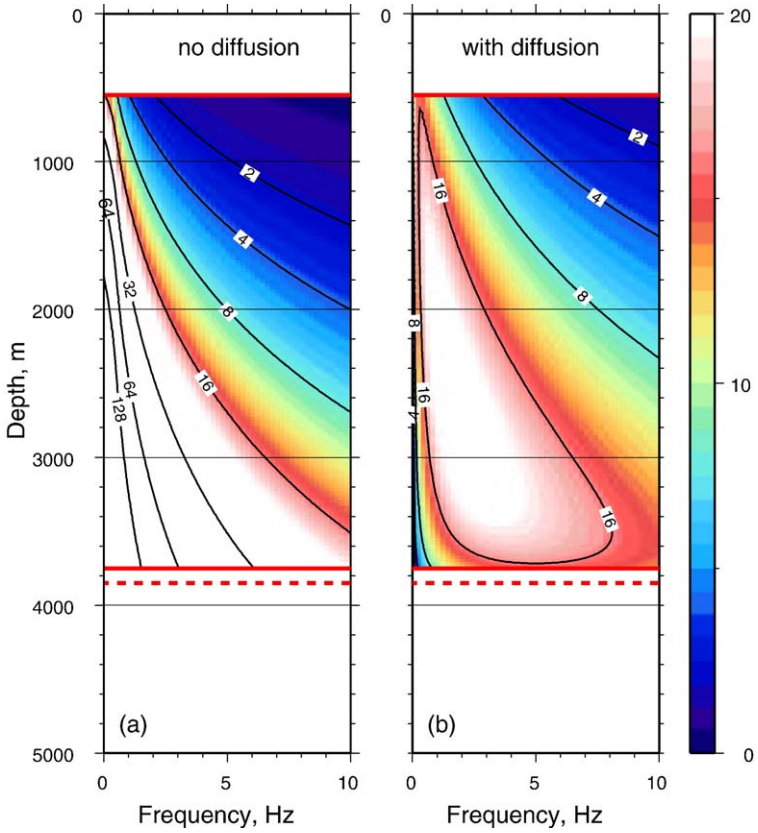


Fig. 9. Comparison of $Q$, (a) calculated assuming bubble growth due to gas expansion alone (no diffusion growth), and (b) $Q$ calculated including bubble growth by diffusion (with diffusion). Input parameters as in Table 1, with $n = 10^{12}$ m$^{-3}$ and $P_{ex}(5000) = 10$ MPa.

mum $Q$ values occurs moves shallower, due to the changes in pressure (Fig. 8 (a)), and hence, this excess pressure needs to be constrained further to allow the depth ranges of resonance to be determined. $Q$ values when including diffusional processes are distinctly lower than when bubble growth is by ideal gas expansion alone, illustrating clearly that by neglecting to include bubble growth by diffusion the ability of seismic waves to propagate within a magma conduit would be over-estimated.

By varying the bubble number density the values of $Q$ within the conduit change noticeably, though the overall dependence on depth and frequency remains unchanged (Fig. 10). The dependence of $Q$ on the bubble number density was discussed earlier, though Fig. 10 shows the extent by which $Q$ could change within a magma conduit depending on this one parameter. To gain a greater understanding of what this means for a propagating wave, the distance an acoustic wave could travel within such magma conduits is calculated (Eq. (3)). We consider the source of the wave to be approximately 1500 m below the surface, as observed in LF event locations at Soufrière Hills Volcano (Neuberg et al., 2006-this issue). The results show that for a conduit with $P_{ex}(5000)=10$ MPa and $n=10^{10}$ m$^{-3}$, a wave with a frequency content of 1–3 Hz, can travel around 1000 m before it becomes damped into the background noise, i.e. when $A(x)=A_o=0.2$ (Fig. 11). LF events have frequencies between 0.2 and 5 Hz (Neuberg et al., 1998), and would propagate in a similar way, with the higher frequencies being damped out after travelling only a short distance. In a magma conduit with a bubble number density of $10^{14}$ m$^{-3}$ and $P_{ex}(5000)=10$ MPa, a wave of frequency 1–3 Hz is completely damped within a few hundred meters, due to the higher attenuation caused by the smaller gas bubbles, and the more prominent diffusion processes. Varying the bubble number density from $10^{10}$ to $10^{14}$ m$^{-3}$ changes the distance a wave could travel from just over a 1000 m to only a few hundred metres.

For resonance to occur within a magma body, a seismic wave must be able to travel multiple times up and down the conduit. The above estimations of travel distances indicate that even if the bubble number den-

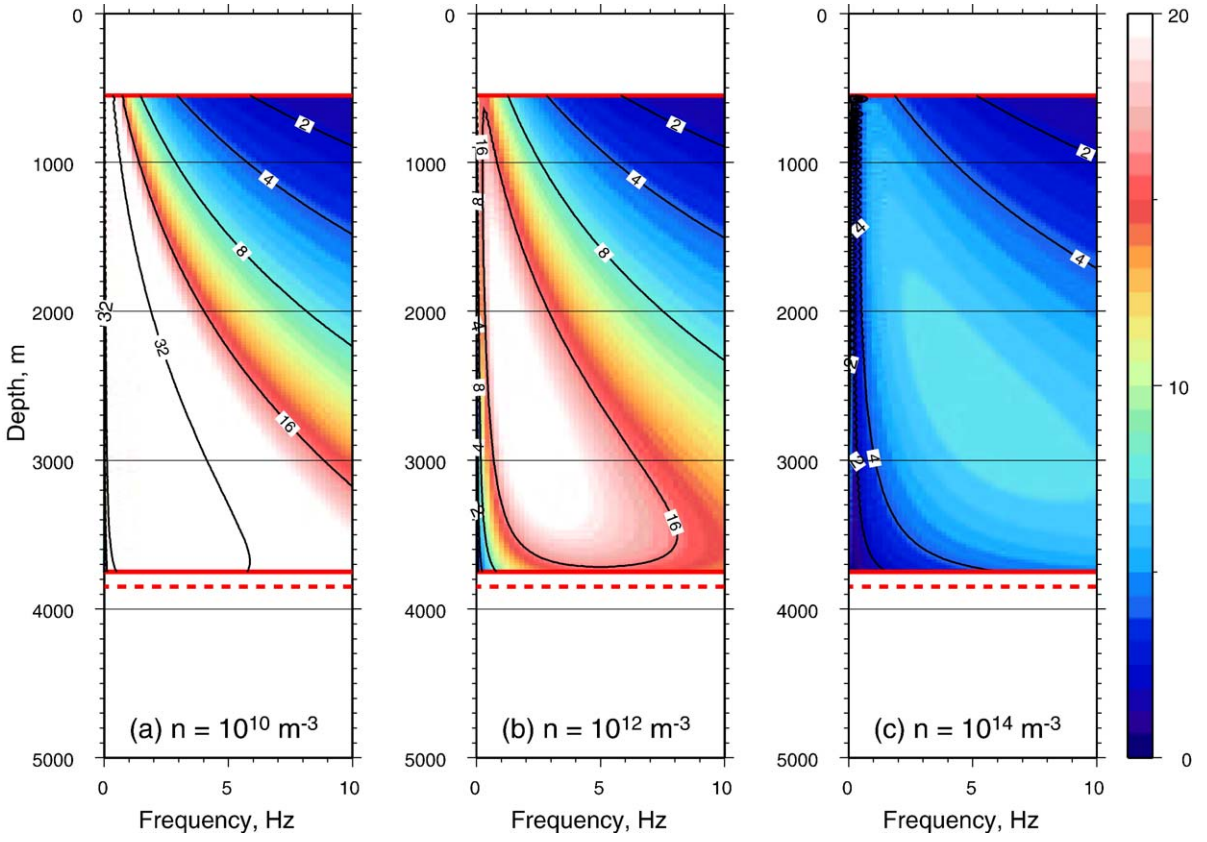


Fig. 10. Variation of $Q$ within a conduit with different bubble number densities, $n=10^{10}$–$10^{14}$ m$^{-3}$. The overall values of $Q$ are noticeably changed by the bubble number density, though the general behaviour remains the same. Input parameters as in Table 1 with $P_{ex}(5000)=10$ MPa.

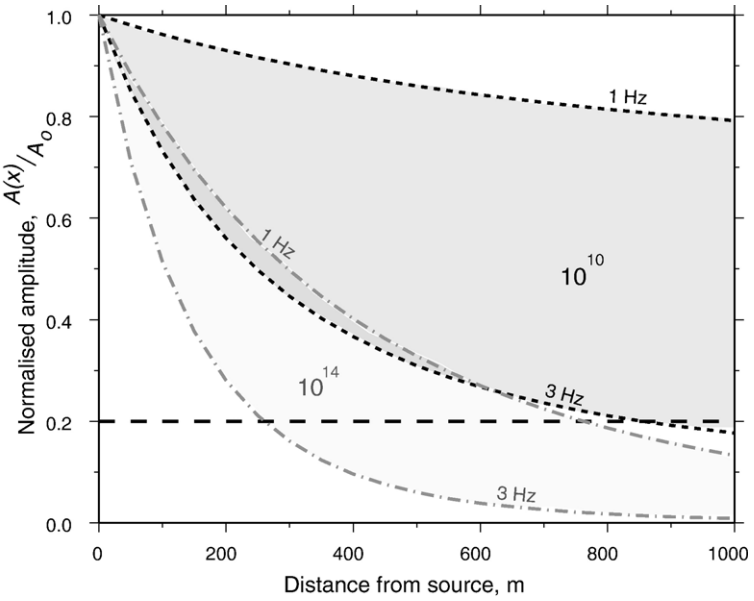


Fig. 11. Distance an acoustic wave (of frequencies 1–3 Hz) could travel within a magma conduit. The seismic source is set to be 1500 m below the surface. Two different bubble number densities are considered, when $n=10^{10}$ m$^{-3}$ (dark shaded area) the wave could travel close to 1000 m before being damped into the background noise ($A(x)=A_o=0.2$). Whereas, when $n=10^{14}$ m$^{-3}$ (light shaded area) the wave is more attenuated, and the wave can only travel a few hundred metres.

sity is as low as $10^{10}$ m$^{-3}$, a seismic wave would not be able to travel multiple times within a 1000 m long conduit and would, therefore, not be able to sustain resonance. Though, it seems possible that resonance could occur within a much shorter conduit section, say of length 200 m, despite the high attenuation levels in magma. An upper limit on the size of the resonating conduit section is proposed to be around a few 100 m, which is in accordance with the low seismic velocities found within the conduit (Fig. 8 (d)).

## 6. Conclusions

In this study we have developed a method of quantifying seismic attenuation in gas-charged magma that reproduces the results of Commander and Prosperetti (1989) and allows the extension of modelling into previously unexplored conditions of bubble growth by diffusion and finite bubble separations. By including bubble growth by diffusion, $Q$ decreased noticeably, implying that growth by diffusion causes more attenuation than growth by gas expansion alone.

Furthermore, when including bubble growth by diffusion the dependence of $Q$ on pressure and frequency becomes more complex due to two factors controlling seismic attenuation. The first is due to the energy dissipation caused by the viscosity of the melt, and the second is due to diffusion processes.

As $Q$ depends on both pressure and frequency, a region of maximum $Q$ exists within the conduit allowing depth ranges where resonance could occur to be identified. The complex dependence of $Q$ with frequency indicates that the spectral content of a seismic signal travelling through such a bubble–melt system would be altered, such that the dominant component would be around 1–2 Hz, which corresponds to the observed frequency contents of LF events on Montserrat (Neuberg, 2000).

The level of attenuation is found to be highly dependent on the size of the bubbles, as indicated by the variation of $Q$ with bubble number density. In this model, we have assumed homogeneous nucleation at one depth, hence, at any given depth above the nucleation level, all the bubbles have the same size. It is likely, however, that bubble nucleate heterogeneously due to the effects of crystals (Hurwitz and Navon, 1994), such that bubbles at the same depth would have a range of sizes. These processes would have a distinct effect on attenuation levels within gas-charged magma conduits, and need to be explored further.

The high attenuation levels (low $Q$) found within gas-charged magmas, when including bubble growth by diffusion, imply that resonance within a conduit of length 1000 m or greater is unlikely. Though a shorter conduit section of around 200 m length could allow resonance and produce LF events like those observed

on Soufrière Hills Volcano, Montserrat. These approximations are determined assuming the waves travel as simple acoustic waves, though it is known that they travel as inhomogeneous interface waves (Ferrazzini and Aki, 1987; Chouet, 1988; Neuberg, 2000). It has been demonstrated that interface waves are dependent on the properties of the surrounding country rock, as well as the magma fluid, and therefore, may be able to travel further than the simple acoustic waves modelled here and allow sustained resonance in longer conduit sections.

Further work is necessary to determine whether resonance is possible within a gas-charged magma conduit, specifically further constraint on input parameters, e.g. bubble number density, is required. Combining the $Q$ models developed here with the finite difference modelling of Jousset et al. (2004) will allow further investigation into interface wave propagation and the ability of a gas-charged magma to sustain resonance.

## Acknowledgements

This work was funded by MULTIMO (EVGI-CT-2000-0021) which is supported by the Environmental and Sustainable Development Program of the European Commission Research Directorate General, a University of Leeds Research Scholarship and BSF 98164. Thanks to the Volcano Seismology Group at the University of Leeds, especially David Green and Susan Sturton for useful discussions and to Peggy Hellweg and an anonymous reviewer for their useful reviews and comments.

## References

Aki, K., Richards, P., 2002. Quantitative Seismology, second edition. University Science Books, Sausalito, California, pp. 161–164.

Aki, K., Fehler, M., Das, S., 1977. Source mechanism of volcanic tremor: fluid driven crack models and their application to the 1963 Kilauea eruption. J. Volcanol. Geotherm. Res. 2, 259–287.

Barclay, J., Rutherford, M., Carroll, M., Murphy, M., Devine, J., 1998. Experimental phase equilibria constraints on pre-eruptive storage conditions of the Soufrière Hills magma. Geophys. Res. Lett. 25 (18), 3437–3440.

Brodsky, E., Sturtevant, S., Kanamori, H., 1998. Earthquakes, volcanoes and rectified diffusion. J. Geophys. Res. 103 (B10), 23827–23838.

Burnham, C., 1975. Water and magmas; a mixing model. Geochim. Cosmochim. Acta 39, 1077–1084.

Carmichael, R., 1990. Physical properties of rocks and minerals. CRC, pages 139 and 429.

Chouet, B., 1988. Resonance of a fluid-driven crack: radiation properties and implications for the source of long-period events and harmonic tremor. J. Geophys. Res. 101, 4375–4400.

Chouet, B., 1996a. Long-period volcano seismicity: its source and use in eruption forecasting. Nature 380, 309–316.

Chouet, B., 1996b. New methods and future trends in seismological volcano monitoring. In: Scarpa, R., Tilling, R. (Eds.), Monitoring and Mitigation of Volcanic Hazards. Springer. Ch. 5.

Chouet, B., Pate, R., Stephens, C., Lahr, J.J.P., 1994. Precursory swarms of long-period events at Redoubt volcano (1989–1990), Alaska: their origin and use as a forecasting tool. J. Volcanol. Geotherm. Res. 62, 95–135.

Christensen, R., 1971. Theory of Linear Viscoelasticity: An Introduction. Academic Press, p. 21.

Commander, K., Prosperetti, A., 1989. Linear pressure waves in bubbly liquids: comparison between theory and experiments. J. Acoust. Soc. Am. 85 (2), 732–746.

Devine, J., Murphy, M., Rutherford, M., Marclay, J., Sparks, R., Carroll, M., Young, S.J.G., 1998. Petrological evidence for pre-eruptive pressure–temperature conditions and recent reheating of andesitic magma erupting at Soufrière Hills Volcano, Montserrat, W.I.. Geophys. Res. Lett. 25 (19), 3669–3673.

Ferrazzini, V., Aki, K., 1987. Slow waves trapped in a fluid-filled crack: implications for volcanic tremor. J. Geophys. Res. 92, 9215–9223.

Futterman, W., 1962. Dispersive body waves. J. Geophys. Res. 67 (13), 5279–5291.

Hess, K.-U., Dingwell, D., 1996. Viscosities of hydrous leucogranitic melts: a non-Arrhenian model. Am. Mineral. 81, 1297–1300.

Hurwitz, S., Navon, O., 1994. Bubble nucleation in rhyolitic melts: experiments at high pressure, temperature, and water content. EPSL 122 (1–3), 267–280.

Jousset, P., Jolly, A., Neuberg, J., 2004. Modelling low-frequency earthquakes in a viscoelastic medium with topography. Geophys. J. Int. 159 (2), 776–802.

Kjartansson, E., 1979. Constant Q-wave propagation and attenuation. J. Geophys. Res. 84 (B9), 4737–4748.

Lahr, J., Chouet, B., Stephens, C., Power, J., Page, R., 1994. Earthquake classification, location, and error analysis in a volcanic environment; implications for the magmatic system of the 1989–1990 eruptions at Redoubt Volcano, Alaska. J. Volcanol. Geotherm. Res. 62, 137–151.

Lensky, N., Lyakhovsky, V., Navon, O., 2001. Radial variations of melt viscosity around growing bubbles and gas overpressure in vesiculating magmas. Earth Planet. Sci. Lett. 186, 1–6.

Lensky, N., Lyakhovsky, V., Navon, O., 2002. Expansion dynamics of volatile-supersaturated liquids and bulk viscosity of bubbly magmas. J. Fluid Mech. 406, 39–56.

Lyakhovsky, V., Hurwitz, S., Navon, O., 1996. Bubble growth in rhyolitic melts: experimental and numerical investigation. Bull. Volcanol. 58, 19–32.

Melnik, O., Sparks, R., 1999. Nonlinear dynamics of lava dome extrusion. Nature 402, 37–41.

Miller, A., Stewart, R., White, R., Luckett, R., Baptie, B., Aspinall, W., Latchman, J., Lynch, L.B.V., 1998. Seismicity associated with dome growth and collapse at the Soufrière Hills Volcano, Montserrat. Geophys. Res. Lett. 25, 3401–3404.

Morrissey, M., Chouet, B., 2001. Trends in long-period seimicity related to magmatic fluid compositions. J. Volcanol. Geotherm. Res. 108, 265–281.

Murphy, M., Sparks, R., Barclay, J., Carroll, M., Lejeune, A., Brewer, T., Macdonald, R., Black, S., Young, S., 1998. The role of magma mixing in triggering the current eruption at the Soufrière Hills Volcano, Montserrat, West Indies. Geophys. Res. Lett. 25, 3433–3436.

Navon, O., Chekhmir, A., Lykhovsky, V., 1998. Bubble growth in highly viscous melts: theory, experiments, and autoexplosivity of dome lavas. Earth Planet. Sci. Lett. 160, 763–776.

Neuberg, J., 2000. Characteristics and causes of shallow seismicity in andesite volcanoes. Philos. Trans. R. Soc. Lond., A 358, 1533–1546.

Neuberg, J., O'Gorman, C., 2002. A model of the seismic wavefield in gas-charged magma: application to Soufrière Hills volcano, Montserrat. In: Druitt, T., Kokelaar, B. (Eds.), The Eruption of Soufrière Hills Volcano, Montserrat, from 1995 to 1999. Geological Society of London Memoir, vol. 21, pp. 603–609.

Neuberg, J., Baptie, B., Luckett, R., Stewart, R., 1998. Results from the broadband seismic network on Montserrat. Geophys. Res. Lett. 25 (19), 3661–3664.

Neuberg, J., Tuffen, H., Collier, L., Green, D.N., Powell, T., Dingwell, D.B., 2006. The trigger mechanism of low-frequency earthquakes on Montserrat. J. Volcanol. Geotherm. Res. 153, 37–50. doi:10.1016/j.jvolgeores.2005.08.008.

O'Connell, R., Budiansky, B., 1978. Measures of dissipation in viscoelastic media. Geophys. Res. Lett. 5 (1), 5–8.

Papale, P., Neri, A., Macedonio, G., 1998. The role of magma composition and water content in explosive eruption: 1. Conduit ascent dynamics. J. Volcanol. Geotherm. Res. 87, 75–93.

Prosperetti, A., Crum, L., Commander, K., 1988. Nonlinear bubble dynamics. J. Acoust. Soc. Am. 83, 502–514.

Rivers, M., Carmichael, I., 1987. Ultrasonic studies of silicate melts. J. Geophys. Res. 92, 9247–9270.

Sparks, R., 1997. Causes and consequences of pressurisation in lava dome eruptions. Earth Planet. Sci. Lett. 150, 177–189.

Sparks, R., Murphy, M., Lejeune, A., Watts, R., Barclay, J., Young, S., 2000. Control on the emplacement of the andesite lava dome of the Soufrière Hills Volcano, Montserrat by degassing-induced crystallization. Terra Nova 12, 14–20.

Stephens, C., Chouet, B., Page, R., Lahr, J., Power, J., 1994. Seismological aspects of the 1989–1990 eruptions at Redoubt Volcano, Alaska: the SSAM perspective. J. Volcanol. Geotherm. Res. 62, 153–182.

Sturton, S., Neuberg, J., 2003. The effects of a decompression on seismic parameter profiles in a gas-charged magma. J. Volcanol. Geotherm. Res. 128, 187–199.

Van Wijngaarden, L., 1968. On the equations of motion for mixtures of liquid and gas bubbles. J. Fluid Mech. 33, 465–474.

Voight, B., Hoblitt, R., Clarke, A., Lockhart, A., Miller, A., Lynch, L., McMahon, J., 1998. Remarkable cyclic ground deformation monitored in real- time on Montserrat, and its use in eruption forecasting. Geophys. Res. Lett. 25 (18), 3405–3408.

Zhang, Y., Behrens, H., 2000. Water diffusion in rhyolitic melts and glasses. Chem. Geol. 169, 306–309.